# Coastal downwelling intensifies landfalling hurricanes

# Supporting Information

Lewis J. Gramer[1,2,*], Jun A. Zhang[1,2], Ghassan Alaka[2], Andrew Hazelton[1,2], Sundararaman Gopalakrishnan[2]

[1] - Cooperative Institute for Marine and Atmospheric Studies, Miami, FL 33149.
[2] - NOAA Atlantic Oceanographic and Meteorological Lab, Miami, FL 33149.

[*] - Corresponding author: Dr. Lewis J. Gramer, 8930 Caribbean Blvd., Cutler Bay, FL 33157. Email: lew.gramer@noaa.gov. Telephone: +1-305-772-7933. ORCID: https://orcid.org/0000-0003-4772-1991

SUBMITTED: Oct 14, 2021
REVISIONS SUBMITTED: Feb 8, 2022
SECOND REVISIONS SUBMITTED: Apr 8, 2022

# Supporting Information

## Additional Details on Methods

The model in these case studies was the quasi-operational Basin-scale HWRF (HWRF-B; Zhang et al. 2016; Alaka et al. 2017, 2019, 2020) developed under HFIP. This model uses a single fixed outer domain, with two TC-following nested domains for each TC of interest. The outermost domain covers approximately a quarter of the globe (from 150°E to 30°E longitude and 35°S to 80°N latitude) and has a horizontal grid spacing of 13.5 km. Two telescopic, storm-following nests are centered on each TC: the outer nest (domain D02) covers 16.5° by 16.5° with horizontal grid spacing of 4.5 km and the inner nest (domain D03) covers 5.5° by 5.5° with horizontal grid spacing of 1.5 km. Up to five sets of nested domains can be deployed for a given initialization time to produce high-resolution forecasts for multiple TCs in the North Atlantic and eastern North Pacific.

With the exceptions noted above, HWRF-B and HWRF are identical in configuration, using the Non-hydrostatic Mesoscale Model (NMM) dynamical core operating on a rotated latitude-longitude Arakawa E-grid. The model has 75 hybrid pressure-sigma vertical levels and a model top of 10 hPa. The 2020 version of HWRF-B used for this study was configured with the Ferrier-Aligo microphysics scheme and the Scale-Aware Simplified Arakawa-Schubert (SASAS) cumulus parameterization scheme. The land-surface model is the Noah LSM and the planetary-boundary layer parameterization is the non-local Hybrid Eddy-Diffusivity Mass-Flux (Hybrid EDMF) scheme. The atmospheric radiation parameterizations are the RRTMG shortwave and longwave radiation schemes.

In all nested domains, a vortex initialization procedure is applied to generate a more realistic TC vortex structure. Depending on the intensity of the TC and the existence of a previous forecast, HWRF-B vortex initialization replaces the initial vortex with one of the following vortices, after correcting for intensity and structure: the previous 6-h HWRF-B forecast, a bogus vortex based on an composite of historical TCs, or the original vortex. Furthermore, the initial vortex is improved by assimilating satellite, airborne, and ground-based observations using a hybrid ensemble-variational system based on gridpoint statistical interpolation (GSI). When airborne tail Doppler radar observations are available for a particular TC, an ensemble of 40 HWRF-B members produces error covariances for use in GSI. Otherwise, HWRF-B GSI uses covariances from an ensemble based on NCEP's Global Forecast System (GFS) that is always available.

HWRF-B is coupled to Message Passing Interface Princeton Ocean Model for Tropical Cyclones (MPIPOM-TC). MPIPOM-TC is based on the three-dimensional, primitive equation ocean model known as the Princeton Ocean Model, and its model description can be found in Yablonsky et al. (2015). The MPIPOM-TC domain for these experiments covers latitudes 5°N to 45°N and longitudes 178°W to 15°W with horizontal resolution 1/12°. Outside of the MPIPOM-TC domain, HWRF-B ingests constant SST from the GFS Analysis. MPIPOM-TC uses terrain-following sigma vertical coordinates ($\boldsymbol{\sigma}$). In the coupled HWRF-B, MPIPOM-TC has 40 full $\boldsymbol{\sigma}$-levels from the sea surface to the seafloor, with higher vertical resolution in the region of the main mixed layer and upper thermocline. The maximum ocean depth for the current configuration is 5500m. The model has a closed boundary condition at the coastline based on a land-sea mask which is consistent with the atmosphere model. The ocean model is initialized from the NCEP Global Real-Time Ocean Forecast System (RTOFS; Mehra and Rivin 2010). In the ocean initialization step, MPIPOM-TC is run for two model days without atmospheric forcing to spin up currents dynamically consistent with the temperature and salinity initialization fields.

For additional information on all of the coupled model configuration details described above, including additional references, please see Alaka et al. (2020).

Three TC case studies from the 2020 North Atlantic hurricane season were evaluated: Sally, Hanna, and Eta. Each TC experienced intensification while approaching land and interacted with the ocean shelf for a period of one day or more. To elucidate processes leading to intensification, model sea-surface fields were analyzed at forecast hours before and immediately after intensification. Supporting Information Table S1 details forecast initialization times for each case and forecast hours chosen for detailed analysis: the forecast hour immediately following intensification and a forecast hour prior to intensification that was near the peak of both air-sea flux and storm kinetic energy (see below). We evaluated the initialization and dynamical evolution of currents and sea temperatures over the shelf in MPIPOM-TC using quality-controlled buoy observations from the NOAA National Data Buoy Center (NDBC 2009; Winant et al. 1994) for one of the case studies, that for TC Sally.

We examined the relationship of air-sea fluxes to total storm kinetic energy and frictional dissipation using a model energy budget following Trenberth (1997) and Kato et al. (2016). Our Equation S1 is the result of integrating Trenberth's (1997) vertically integrated Eq. 16 over the inner TC domain.

$$\left[\iint\int_0^{p_s} KE\ dp\ dA\right]_{t0}^{tH} + \int_{t0}^{tH}\iint\int_0^{p_s} \nabla_p \cdot \vec{\boldsymbol{U}}\, KE\ dp\ dA\ dt - \left[\iint\int_0^{p_s} (c_pT + Lq + \Phi_s) dp\ dA\right]_{t0}^{tH} - \int_{t0}^{tH}\iint\int_0^{p_s} \nabla_p \cdot \vec{\boldsymbol{U}}(c_pT + Lq + \Phi) dp\ dA\ dt + g\ RHF + g\ (THF_d + THF_s) - FD = 0 \qquad (1)$$

Eq. S1 includes terms for air pressure $p$, surface air pressure $p_s$, kinetic energy $KE$, storm domain area element $A$, forecast initialization time $t_0$ and forecast valid time $t_H$, wind velocity $\boldsymbol{U}^{\rightarrow}$, specific heat capacity of air $c_p$, air temperature $T$, latent heat of evaporation $L$, specific humidity $q$, geopotential at the surface $\phi_s$ and throughout the storm $\phi$, respectively, gravitational acceleration $g$, net radiative heat flux $RHF$, net turbulent air-sea enthalpy flux over deep water $THF_d$ and over the shelf $THF_s$, and frictional dissipation $FD$ at the surface. Area element $A$ is taken to consist of the region of instantaneous 17.5 $ms^{-1}$ (34 kt) winds within the innermost domain (e.g., Figure 1). Square brackets denote differences between instantaneous values evaluated at different forecast hours.

We follow Emanuel (1986) and Wang and Xu (2010) in considering a simplified version of the above energy budget consisting of only the terms highlighted in red. This simplified equation elucidates the relationship between TC intensity change and TC interaction with the ocean and allows for the analysis of surface enthalpy fluxes over the shelf as a separate contribution to the budget. This study considers turbulent air-sea enthalpy fluxes only at gridpoints where 10 m winds are 17.5 $ms^{-1}$ or greater. Fluxes within atmospheric grid cells over ocean model topography of 150 m depth or less are summed in the $THF_s$ term; all other air-sea enthalpy fluxes are accumulated in $THF_d$. Frictional dissipation (*FD*) is estimated from predicted 10 m wind speeds as per Kato et al. (2016). We calculate total kinetic energy averaged over all vertical levels in the inner atmospheric model domain. All other terms in Eq. S1 (terms in black) are treated as residuals.

## Additional Figures

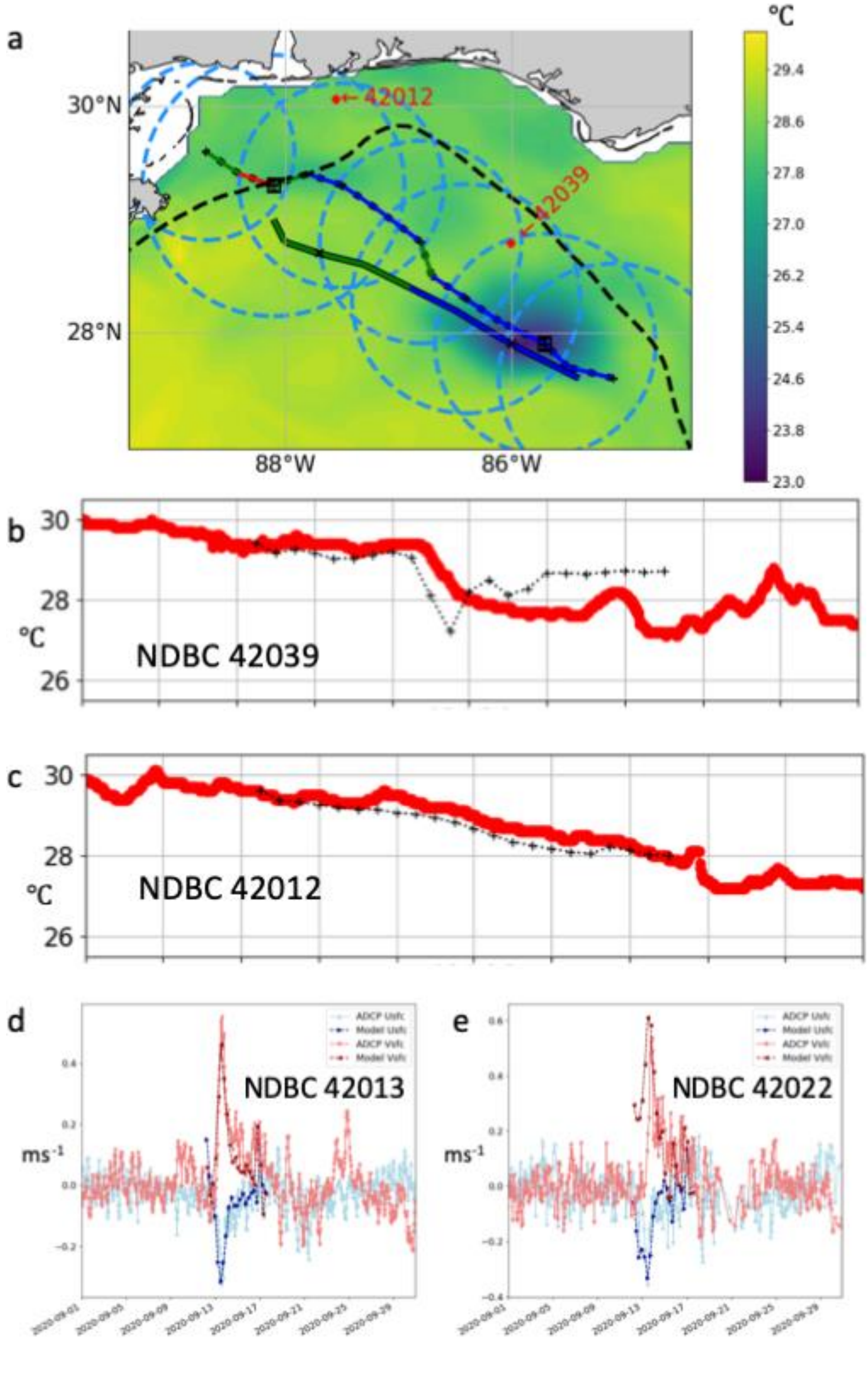

Figure S1: Data from NOAA NDBC buoys in the Gulf of Mexico for 10-20 Sep 2020: (a) map showing model SST [ºC] for forecast hour 54, together with location of buoys (red dots) along Sally's HWRF-B forecast track (dashed outline, colored by storm intensity) and 17.5 $ms^{-1}$ wind radii (circles). Best track is also outlined with solid black. Model 150 m isobath is a dashed black line. (b) Near-surface sea temperature (ºC; red) compared with model SST (dotted black "+") for buoy 42039 in the deeper Gulf, water depth 281 m. (c) Near-surface temperature and model SST for buoy 42012 on the northern Gulf shelf in 24 m of water. (d) Near-surface currents [m/s] west-to-east across-shore (u, blue) and south-to-north alongshore (v, red); solid lines show quality-controlled ADCP measurements (top good bin) from two buoys on west Florida shelf, dashed lines show ocean model output (topmost model level).

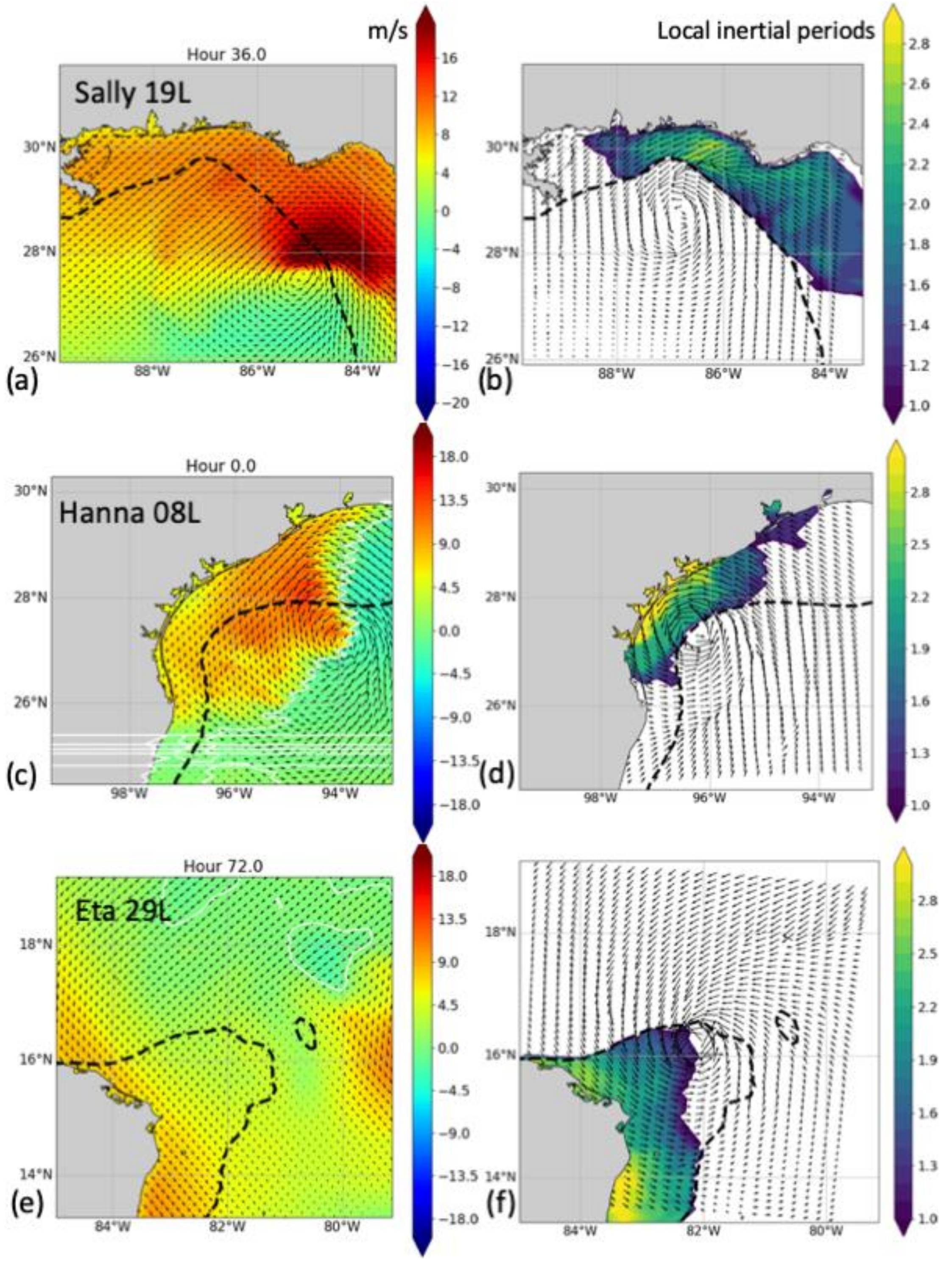


Figure S2: (a,c,e) Snapshot of wind vectors and magnitude of downwelling-favorable wind component (alongshore $ms^{-1}$; shading, with zero contour marked in white) at a forecast hour one inertial period prior to intensification; (b,d,f) Wind vectors at hour just prior to intensification, and accumulated number of inertial periods (multiples of 22 h at the latitude of Sally and Hanna, 42 h for Eta; shading) during which downwelling-favorable winds were blowing over the shelf. Thick dashed black line shows the 150 m isobath outlining the shelf regions; land is in gray.

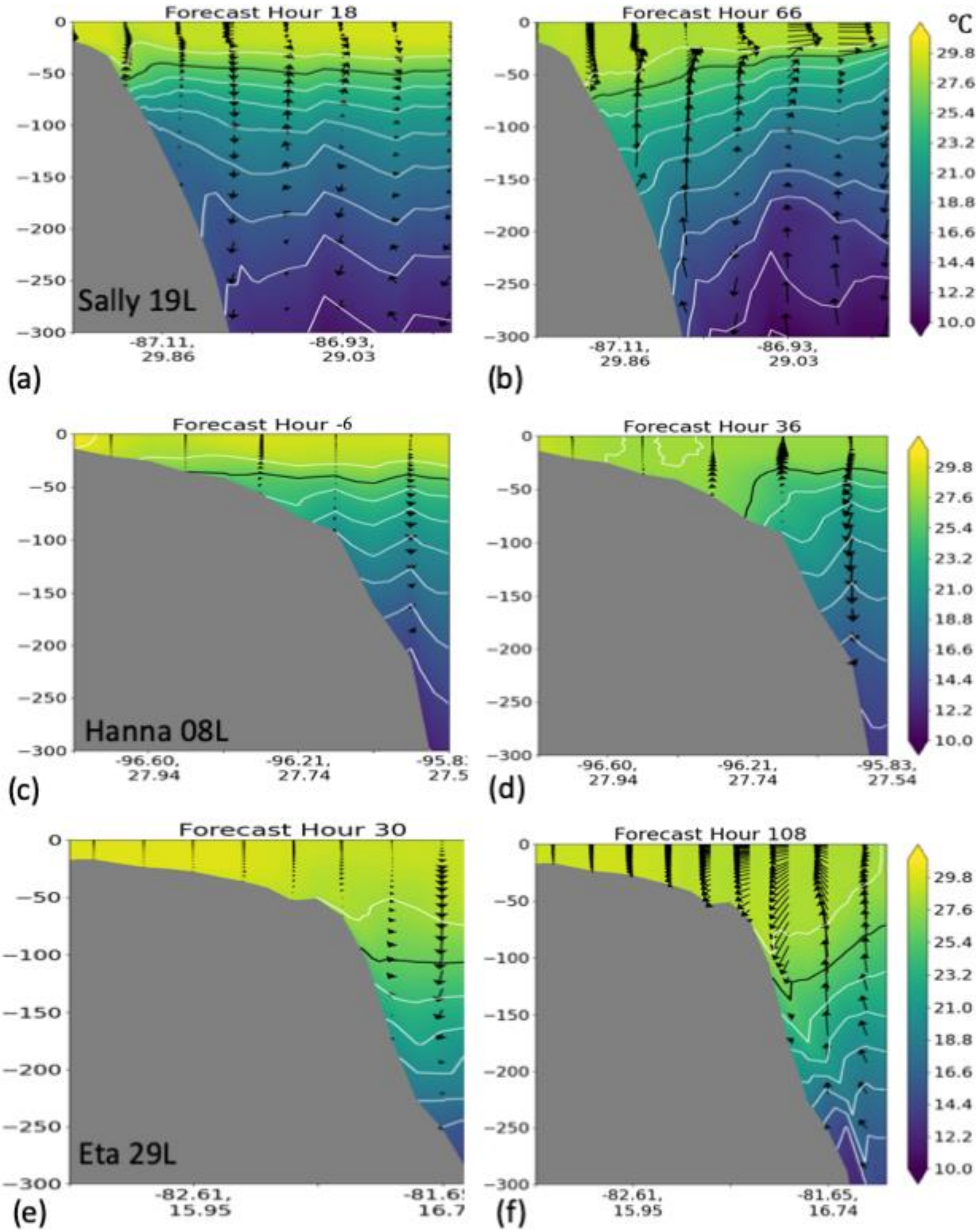


Figure S3: Section plots (along the same section lines shown in Figure 2, middle panel), shown here at two other times separated from each other by two local inertial periods. These show the evolution of the downwelling circulation cell (currents in black arrows) and depression of isotherms (sea temperature in ºC) over the shelf that formed ahead of the passage of each TC.

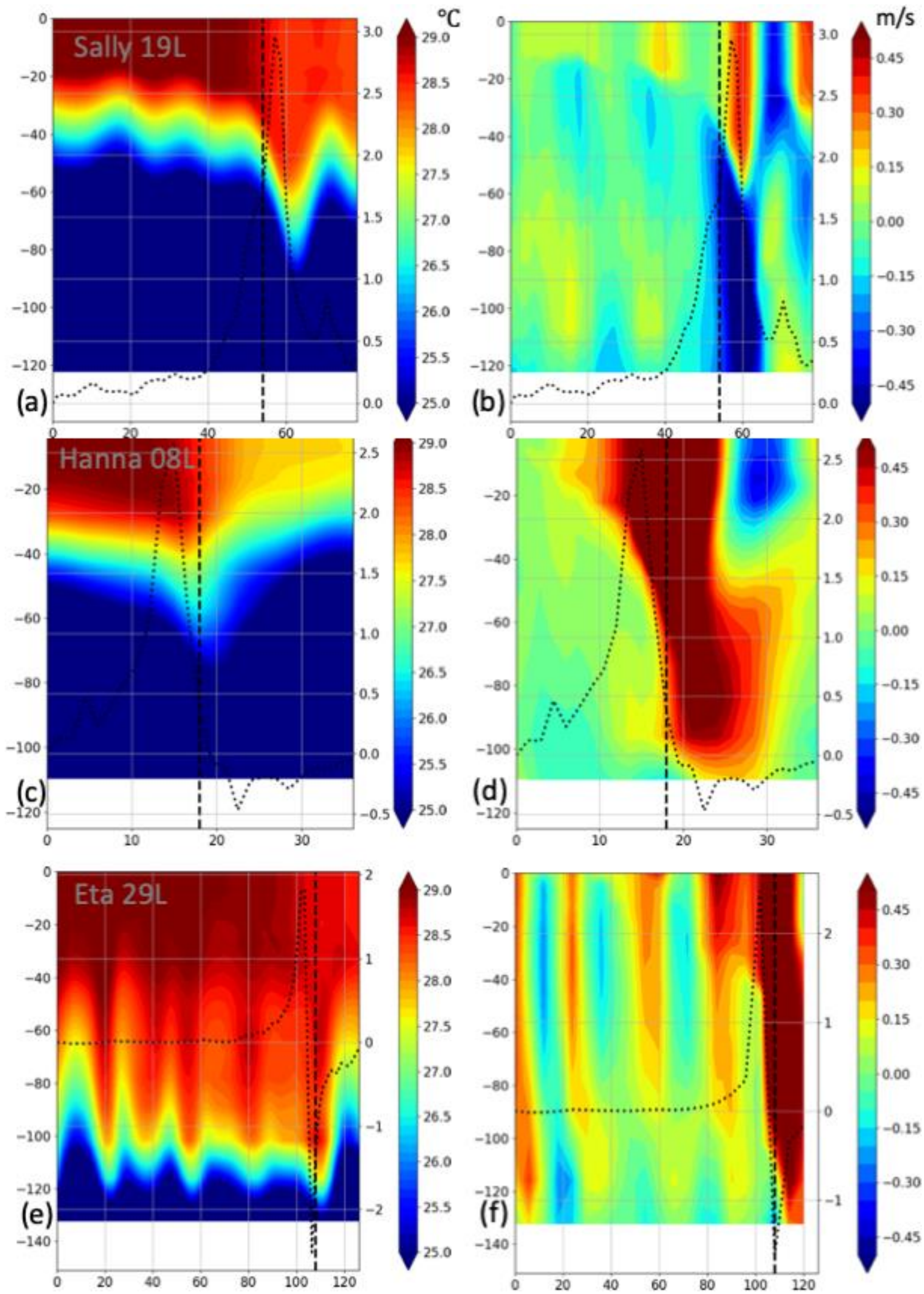


Figure S4: Hovmöller diagrams showing change in vertical ocean profiles at a point near the 150 m isobath along each of the onshore tracks in the left and middle panels of Figure 2. (a,c,e) Ocean temperature [ºC] and (b,d,f) cross-shelf currents [m/s]. The right axis and black dotted line show along-shore 10 m wind stress from the model [N/m$^2$]. Dashed vertical black line shows the forecast hour highlighted in Figure 2 and in the left panels of Figures 1, 3, and 4.

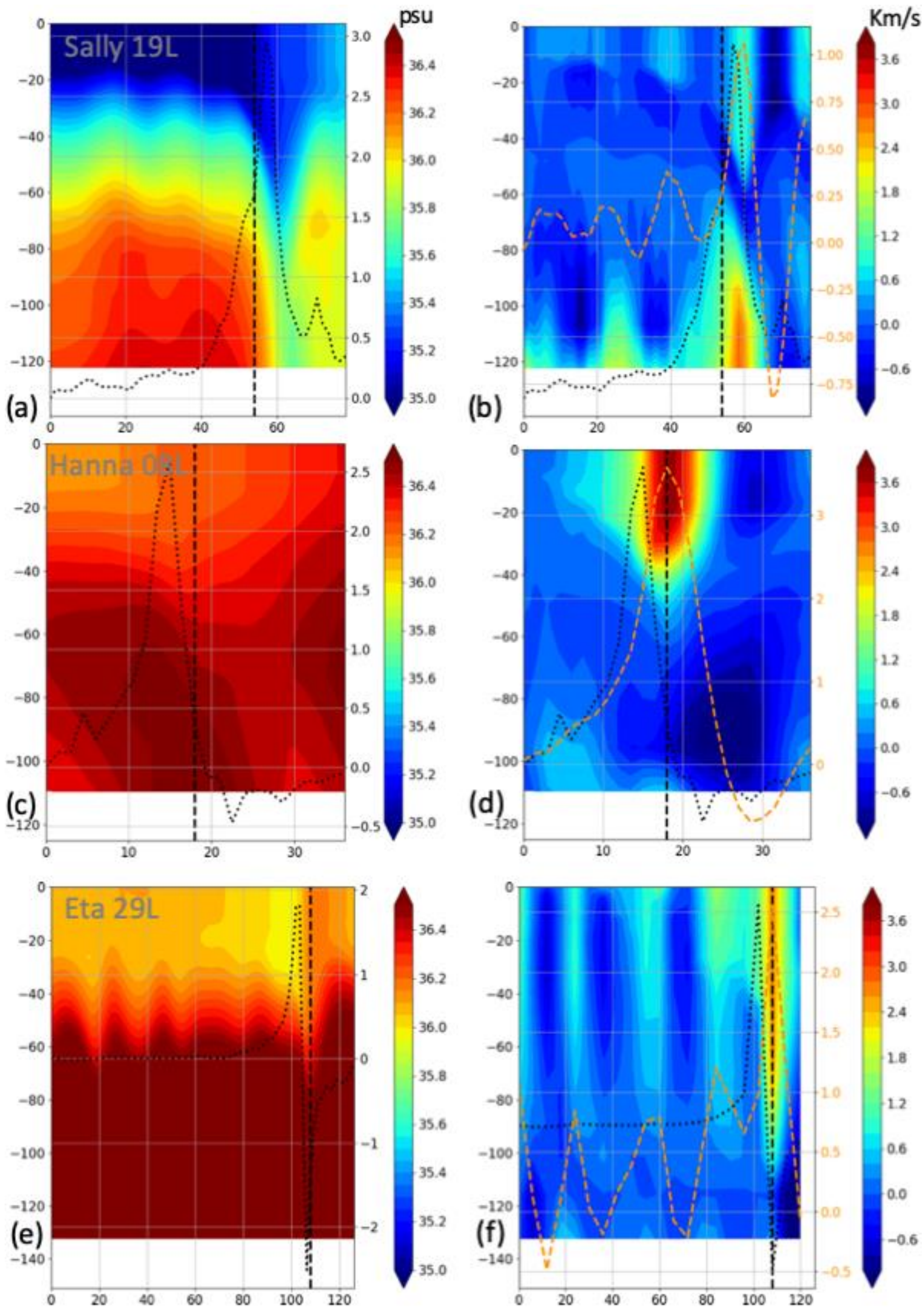


Figure S5: Hovmöller diagrams similar to those in Figure S4, showing changes in: (a,c,e) salinity [psu] and (b,d,f) cross-shore heat transports [K·m/s]. For left-hand panels, right axis and black dotted line show alongshore 10 m wind stress from the model [N/m$^2$]. For right-hand panels, black dotted line still shows along-shore wind stress but with no corresponding axis, while the dashed orange line and right axis show cross-shore net heat flux [MW/m$^2$] relative to 26 °C.

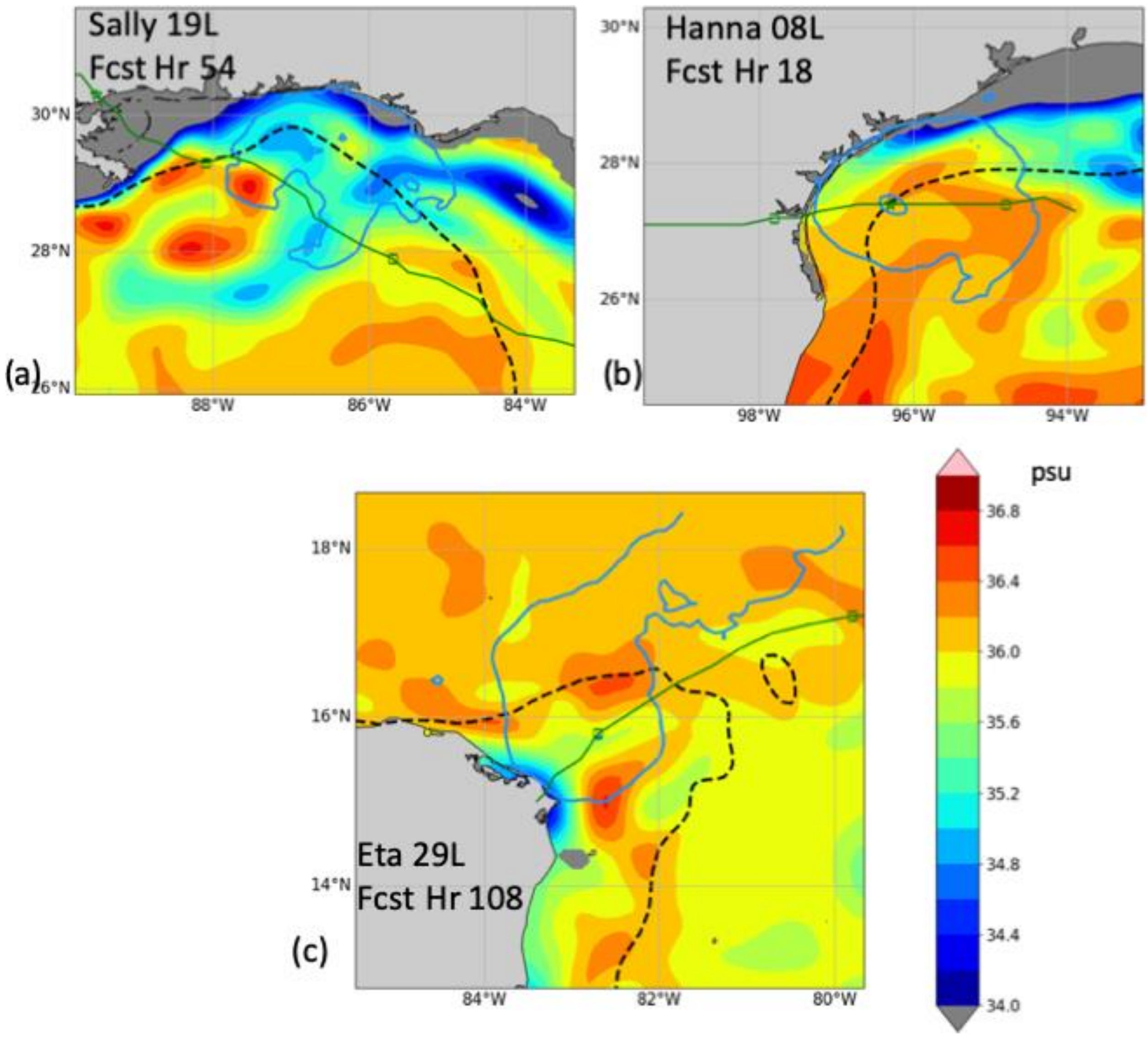


Figure S6: Model sea-surface salinity (psu; shading) at forecast hour just prior to intensification for each of the three case studies. Contour of winds > 17.5 m/s (blue) and the 150 m isobath (black dashed), and forecast TC track and positions (green lines and squares) as in Figures 1-3.

Table S1: Storm forecast initialization time, forecast hours (chosen before and after intensification) that are highlighted in Figs.1-4, peak intensity change in the 24 h following the first highlighted forecast hour, and environmental characteristics during the highlighted period: environmental deep vertical wind shear (200-850 mbar), translation speed of the storm, total air-sea enthalpy flux (THF), and percentage of THF deriving from shelf waters.

| **Storm** | **Forecast Init. Time** | **Fcst. Hours Highlighted** | **Forecast Intensity Change in 24 h; $ms^{-1}$** | **Environ. Shear; $ms^{-1}$; Direction** | **Fcst. Storm Transl. Speed; $ms^{-1}$; Dir.** | **Total Air-Sea Heat Flux (THF); TJ** | **% THF from shelf** |
|---|---|---|---|---|---|---|---|
| Sally 19L | 0600Z 12 September 2020 | 54, 66 | +26 | 13 WSW | 3.0 SE | $1.0 \times 10^7$ | 60% |
| Hanna 08L | 1800Z 24 July 2020 | 18, 24 | +18 | 5.1 NW | 4.1 E | $3.5 \times 10^6$ | 80% |
| Eta 29L | 0600Z 30 October 2020 | 108, 114 | +11 | 8.7 S | 3.6 NE | $1.8 \times 10^7$ | 40% |